Mathematical Analysis of the Photo-Acoustic Imaging Modality Using Dielectric Nanoparticles

Mourad Sini

Johann Radon Institute for Computational and Applied Mathematics (RICAM)
Austrian Academy of Sciences (ÖAW)
Linz, Austria

Online Talk at S.T. Yau Center of Southeast University
June 25th, 2020

Supported by **FWF: P 30756-NBL**

Outline

1. Motivation-why contrast agents?
2. Characterization of the key resonances
3. Acoustic imaging with resonating bubbles
4. Photo-Acoustic imaging with resonating nanoparticles

Introduction and motivation

1. Conventional imaging techniques, as in microwave imaging, are known to be capable of extracting features in breast cancer, for instance, in case of the relatively high contrast of the permittivity [1].

2. However, in case of benign tissue the variation of the permittivity is quite low so that such modalities are limited to be used for early detection.

Creating such missing contrasts is highly desirable. One way to do it is to use:

(1). Electromagnetic Nanoparticles. [2]

(2). Micro-Bubbles. [3]

---

1 G. Belizzi and O. M. Bucci. Microwave cancer imaging exploiting magnetic nanaparticles as contrast agent. IEEE Transactions on Biomedical Engineering, (2011).

2 idem

3 S. Qin, C. F. Caskey and K. W. Ferrara. Ultrasound contrast microbubbles in imaging and therapy: physical principles and engineering. Phys Med Biol. (2009).

Noninvasive photoacoustic imaging of a rat's cerebral cortex using nanoparticles as contrast agents.

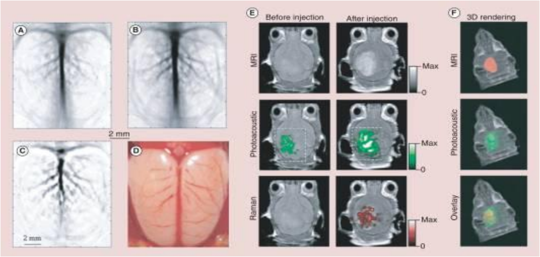

From: W. Li and X. Chen, Gold nanoparticles for photoacoustic imaging. Nanomedicine (Lond). 2015 Jan; 10(2): 299–320.

(a). Multilocular pancreatic cystic mass revealing intracystic septal enhancement 45 s after microbubble injection with Ultrasound. (b). The pattern is confirmed at contrast-enhanced CT.

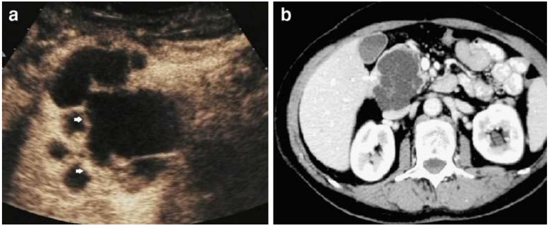

From: E. Quaia, Eur Radiol (2007) 17: 1995–2008

Characterization of these contrast agents I:

Electromagnetic Nanoparticles

We call $(D_m, \varepsilon_m, \mu_m)$ an electromagnetic nanoparticle of shape D_m, diameter a of order of few tens of nanometers and permittivity and permeability ε_m, μ_m respectively.

We call them

1. **Electric (or Dielectric) Nanoparticles** if in addition: $\frac{\varepsilon_m}{\varepsilon_0} \sim a^{-\alpha}, \alpha > 0$ and $\frac{\mu_m}{\mu_0} \sim 1$ as $a \ll 1$.

This implies that the relative index of refraction is large, i.e. $\frac{\kappa_m^2}{\kappa_0^2} := \frac{\varepsilon_m \mu_m}{\varepsilon_0 \mu_0} \gg 1$ as $a \ll 1$. Hence the relative speed of propagation $\frac{c_m}{c_0} := \frac{\kappa_0}{\kappa_m}$ is small. But, the contrast of the transmission coefficient is moderate.

2. **Magnetic (or Plasmonic) Nanoparticles** if in addition $\frac{\varepsilon_m}{\varepsilon_0} \sim 1$ and $\frac{1}{2} \frac{\mu_m+\mu_0}{\mu_m-\mu_0}$ is “very close” to one of the eigenvalues of the Neumann-Poincaré operator (i.e. the adjoint of the double layer operator). This means that the relative speed of propagation is moderate. But the contrast of the transmission coefficient is large.

Note that the coefficients with zero as subscripts refer to the background media.

Characterization of these contrast agents II:

Micro-Bubbles

We call (D_m, ρ_m, k_m) a micro-bubble of shape D_m, diameter a, of about few tens of micrometers, and mass density and bulk modulus ρ_m, k_m respectively.

They are called

1. **Low Dense / Low Bulk Bubbles** if in addition: $\frac{\rho_m}{\rho_0} \sim a^\alpha$ and $\frac{k_m}{k_0} \sim a^\alpha$ with $\alpha > 0$ and then $\frac{c_m^2}{c_0^2} := \frac{\rho_m}{\rho_0} \frac{k_m}{k_0} \sim 1$ as $a \ll 1$. This means that the relative speed of propagation $\frac{c_m^2}{c_0^2}$ is moderate. But the contrast of the transmission coefficient is large.

2. **Moderate Dense / Low Bulk Bubbles** if in addition: $\frac{\rho_m}{\rho_0} \sim 1$ and $\frac{k_m}{k_0} \sim a^{-\alpha}, \alpha > 0,$ as $a \ll 1$. This means that the relative speed of propagation is small. [4] But the contrast of the transmission coefficient is moderate.

Note that the coefficients with zero as subscripts refer to the background media.

[4] Such bubbles are not known to exist in nature but they might be designed, see the following work: F. Zangeneh-Nejad and R. Fleury, Acoustic Analogues of High-Index Optical Waveguide Devices. Sci Rep 8, 10401 (2018).

Key Resonances

Some related resonances

These differences give rise to different types of resonances:

Micro-bubbles

1. the Minnaert resonance for the **Low Density** / **Low Bulk bubbles**. A surface-mode.
2. A sequence of resonances for the **Moderate Density** / **Low Bulk bubbles**. Body-modes.

Nanoparticles

1. the plasmonic sequence of resonances for **plasmonic nanoparticles**. Surface-modes.
2. the Mie (or dielectric) sequence of resonances for the **dielectric nanoparticles**. Body-modes.

Formal characterization of the resonances-Acoustic case

Let $D = z + a\,B$ be a bounded, smooth and connected subset of $\mathbb{R}^3$, with a 'radius' $a \ll 1$. Let $u = u^s + u^i$ be the solution of the acoustic scattering problem

$$\begin{cases} \operatorname{div} \frac{1}{\rho} \nabla u + \omega^2 \frac{1}{k} u = 0 \quad \text{in } \mathbb{R}^3, \\ \\ u^s := u - u^i \text{ satisfies the Sommerfeld Radiation Conditions (S.R.C.)} \end{cases} \tag{2.1}$$

where

$$\rho := \begin{cases} \rho_1 & \text{inside } D, \\ \\ \rho_0 & \text{outside } D \end{cases} \qquad and \qquad k := \begin{cases} k_1 & \text{inside } D, \\ \\ k_0 & \text{outside } D. \end{cases} \tag{2.2}$$

Here $u^i := u^i(x, \omega, d) := e^{i\omega\sqrt{\frac{\rho_0}{k_0}}\, x \cdot \theta}$ is any incident plane wave propagating in the direction θ.

From the Lippmann-Schwinger representation we have

$$u(x) - \alpha \operatorname{div}_x \int_D G_\omega(x-y)\nabla u(y)dy - \beta\omega^2 \int_D G_\omega(x-y)u(y)dy = u^i(x), \tag{2.3}$$

where $\alpha := \frac{1}{\rho_1} - \frac{1}{\rho_0}$ and $\beta := \frac{1}{k_1} - \frac{1}{k_0}$.

By integration by parts, (2.3) becomes

$$u(x) - \gamma\omega^2 \int_D G_\omega(x-y)u(y)dy + \alpha \int_{\partial D} G_\omega(x-y)\frac{\partial u}{\partial \nu}(y)dy = u^i(x), \tag{2.4}$$

where $\gamma := \beta - \alpha\rho_1/k_1$. In addition

$$(1+\frac{\alpha}{2})\frac{\partial u}{\partial \nu} - \gamma\omega^2 \partial_{\nu-} \int_D G_\omega(x-y)u(y)dy + \alpha(K_D^\omega)^*[\frac{\partial u}{\partial \nu}] = \frac{\partial u^i}{\partial \nu}. \tag{2.5}$$

Hence for $x \in \mathbb{R}^3 \setminus \overline{D}$, $u(x)$ is characterized by $u|_D$ and $\frac{\partial u}{\partial \nu}|_{\partial D}$ which are solutions of the system:

$$[I - \gamma\omega^2 N_\omega]u + \alpha \int_{\partial D} G_\omega(x-y)\frac{\partial u}{\partial \nu}(y)dy = u^i(x), \text{ in } D \tag{2.6}$$

$$[\frac{1}{\alpha} + \frac{1}{2} + (K_D^\omega)^*][\frac{\partial u}{\partial \nu}] - \frac{\gamma}{\alpha}\omega^2 \partial_{\nu_-} \int_D G_\omega(x-y)u(y)dy = \frac{1}{\alpha}\frac{\partial u^i}{\partial \nu}, \text{ on } \partial D \tag{2.7}$$

with the Newtonian (a volume-type) operator:

$$N_\omega : L^2(D) \longrightarrow H^2(D), \quad N_\omega(u)(x) := \int_D G_\omega(x-y)u(y)dy$$

and the Neumann-Poincaré (a surface-type) operator

$$(K_D^\omega)^* : H^{-1/2}(\partial D) \longrightarrow H^{-1/2}(\partial D), \quad (K_D^\omega)^*(f)(x) := pv. \int_{\partial D} \frac{\partial}{\partial \nu_x} G_\omega(x-y)f(y)dy.$$

Key property: For $\omega = 0$, each of these operators generates a sequence of eigenvalues: $\lambda_m(N_0) \overset{m\to\infty}{\longrightarrow} 0$ and $\sigma_p((K_D^0)^*) \subset (-\frac{1}{2}, \frac{1}{2})$. In addition, we have $K_D^0(1) = -\frac{1}{2}$. These singular values are behind all the used resonances.

Indeed!

$$[I-\gamma\,\omega^2\;N_\omega]u+\alpha\int_{\partial D}G_\omega(x-y)\frac{\partial u}{\partial \nu}(y)dy=u^i(x),\ \text{ in } D \tag{2.8}$$

$$[\frac{1}{\alpha}+\frac{1}{2}+(K_D^\omega)^*][\frac{\partial u}{\partial \nu}]-\frac{\gamma}{\alpha}\omega^2\partial_{\nu_-}\int_D G_\omega(x-y)u(y)dy=\frac{1}{\alpha}\frac{\partial u^i}{\partial \nu},\ \text{ on } \partial D. \tag{2.9}$$

1. For **Low Density / Low Bulk bubbles**, we have $\gamma\sim 1$ and then $\gamma\omega^2 N_\omega \ll 1$ as $a\ll 1$. But as $\alpha\gg 1$, precisely if $\alpha\sim a^{-2}$ as $a\ll 1$, then we can excite the eigenvalue $-\frac{1}{2}$ of K_D^0. In this case, we have the Minnaert resonance with surface-modes. [5]

2. For **Moderate Density / Low Bulk bubbles**, we have $\alpha\sim 1$ and then we keep away from the full spectrum of $(K_D^0)^*$. But as $\gamma\sim a^{-2}\gg 1$, we can excite the eigenvalues of the Newtonian operators N_0. This gives us a sequence of resonances with volumetric-modes.

Using Lippmann-Schwinger equations allows to characterize all these resonances and for varying backgrounds. [6]

---

5 First observed by H. Ammari, B. Fitzpatrick, D. Gontier, H. Lee, and H. Zhang. Minnaert resonances for acoustic waves in bubbly media. (2018).

6 A. Dabrowski, A. Ghandriche and M. Sini, Mathematical analysis of the acoustic imaging modality using bubbles as contrast agents at nearly resonating frequencies. arXiv:2004.07808.

Formal characterization of the resonances-Electromagnetic case

We deal with non-magnetic materials. The electric field $E = E^s + E^i$ is solution of the electromagnetic scattering problem

$$\begin{cases} curl\ curl\ E + \omega^2 \varepsilon \mu_0 E = 0 \quad \text{in } \mathbb{R}^3, \\ E^s \text{ satisfies the S-M.R.C.} \end{cases} \tag{2.10}$$

where

$$\varepsilon := \begin{cases} \varepsilon_1 & \text{inside } D, \\ \varepsilon_0 & \text{outside } D. \end{cases} \tag{2.11}$$

Here E^i is a polarized incident electric field propagating in the background medium.

The corresponding Lippmann-Schwinger equation is:

$$E(x) - \eta \operatorname{div}_x \int_D \nabla G_\omega(x-y) \cdot E(y)dy - \omega^2 \eta \int_D G_\omega(x-y)E(y)dy = E^i(x), \tag{2.12}$$

where $\eta = \varepsilon_1 - \varepsilon_0$.

By integration by parts, (2.12) becomes

$$E(x) - \eta\omega^2 \int_D G_\omega(x-y)E(y)dy + \eta\nabla \int_{\partial D} G_\omega(x-y)E \cdot \nu(y)dy = E^i(x). \tag{2.13}$$

In addition

$$(1+\frac{\eta}{2})E \cdot \nu - \eta\mu_0\omega^2 \nu \cdot \int_D G_\omega(x-y)E(y)dy + \eta(K_D^\omega)^*[E \cdot \nu] = E^i \cdot \nu, \text{ on } \partial D. \tag{2.14}$$

Hence for $x \in \mathbb{R}^3 \setminus \overline{D}$, $E(x)$ is characterized by $E|_D$ and $E \cdot \nu|_\partial D$ which are solutions of the system:

$$[I - \eta\omega^2 N_\omega]E + \eta\nabla \int_{\partial D} G_\omega(x-y)E\cdot\nu(y)dy = E^i(x), \text{ in } D \tag{2.15}$$

$$[\frac{1}{\eta} + \frac{1}{2} + (K_D^\omega)^*][E\cdot\nu] - \omega^2\nu\cdot\int_D G_\omega(x-y)E(y)dy = \frac{1}{\eta}E^i\cdot\nu, \text{ on } \partial D. \tag{2.16}$$

1. For **dielectric nanoparticles**, we have $\eta \gg 1$. Hence $\frac{1}{\eta} \ll 1$, however we keep away from the full spectrum of $(K_D^0)^*$ as the sources are average-zero. But if in addition $\eta \sim a^{-2} \gg 1$, then we can excite the eigenvalues of the Newtonian operators N_0. This gives us the sequence of Mie (or dielectric) resonances. [7]

2. Observe that if η is negative (i.e. **negative permittivity**) then we can excite the sequence of eigenvalues of $(K_D^0)^*$. This gives us the sequence of electric plasmonics. [8]

7 Published, for scalar waves, in T. Meklachi, S. Moskow, and J.C. Schotland, (2018) and in H. Ammari, A. Dabrowski, B. Fitzpatrick, P. Millien, and M. Sini (2019).

8 Studied in a **series** of works by H. Ammari et al. using boundary integral equations (i.e. indirect methods).

Summary on the existence of the resonances

1. Acoustic bubbles:

   - For **Low Density / Low Bulk bubbles**, we have the Minnaert resonance with surface-modes.
   - For **Moderate Density / Low Bulk bubbles**, we have a sequence of resonances with volumetric-modes.

2. Electromagnetic nanoparticles:

   - For **dielectric nanoparticles**, we have the sequence of Mie (or dielectric) resonances with volumetric-modes.
   - For **negative (real part of the) permittivity**, we have the sequence of plasmonic resonances with surface-modes.

Acoustic Imaging Using Resonating Bubbles

Expansion of the fields: Single bubble case-I

Let $D := z + a\,B$ be the bubble of center z injected in the body to image Ω.

Let $V := V^s + V^i$ be the total field generated by the background (ρ_0, k_0) without the bubble.

We set $U := U^s + U^i$ be the total field generated by the background (ρ, k) in the presence of one bubble.

Here $V^i = U^i := e^{i\kappa_0 \theta \cdot x}$ be the incident plane wave where $\kappa_0 := \omega\sqrt{\frac{\rho_{0,\infty}}{k_{0,\infty}}}$ and θ is the direction of incidence.

Expansion of the fields: Single bubble case-II

Recall the acoustic model:

$$\begin{cases} \text{div}\, \frac{1}{\rho} \nabla U + \omega^2 \frac{1}{k} U = 0 \quad \text{in } \mathbb{R}^3, \\ U^s := U - U^i \text{ satisfies the Sommerfeld Radiation Conditions (S.R.C.)} \end{cases} \tag{3.1}$$

where

$$\rho := \begin{cases} \rho_1 & \text{inside } D, \\ \rho_0 & \text{outside } D \end{cases} \quad \textit{and} \quad k := \begin{cases} k_1 & \text{inside } D, \\ k_0 & \text{outside } D \end{cases} \tag{3.2}$$

and ρ_0 and k_0 are variable coefficients which are constant outside the target domain Ω.

Here we take the scales $k_1 := \bar{k}_1\, a^2$ and $\rho_1 := \bar{\rho}_1\, a^2$.

With these scales, we have existence of the Minnaert resonance.

Expansion of the fields: Single bubble case-III

We have the expansion:

$$U^\infty(\hat{x},\theta,\omega) = V^\infty(\hat{x},\theta,\omega) - \frac{1}{\overline{k_1}}\,\frac{\omega_M^2}{\omega^2-\omega_M^2}\,|B|\; a\, V(z,-\hat{x},\omega)\; V(z,\theta,\omega) + O(a) \tag{3.3}$$

where $k_1 = \overline{k_1}\; a^2$, and

$$\omega_M = \omega_M(z) := \sqrt{\frac{\overline{k_1}/\rho_0(z)}{A_{\partial B}}} \qquad (\textit{ The Minnaert resonance!}) \tag{3.4}$$

with $A_{\partial B} := -\int_{\partial B}\int_{\partial B} \frac{(x-y)\cdot\nu(x)}{4\pi|x-y|}\,dxdy$.

Solution of the inverse problem using one bubble-I

We use as data the multiple frequencies backscattered fields:

$$U^{\infty}(-\theta, \theta, \omega)$$

with one incident direction θ and a band of frequencies

$$[\omega_M^{min}, \ \omega_M^{max}]$$

where

$$\omega_M^{min} < \sqrt{\frac{\overline{k_1}}{\left(\max_\Omega \rho_0(z)\right) \ A_{\partial B}}} \text{ and } \omega_M^{max} > \sqrt{\frac{\overline{k_1}}{\left(\min_\Omega \rho_0(z)\right) \ A_{\partial B}}}.$$

Solution of the inverse problem using one bubble-II

1. We have the property: $|U^\infty(-\theta,\theta,\omega)| \gg 1 \Longleftrightarrow \omega \sim \omega_M(z)$. From this, we recover the function $\omega_M(z),\ z\in\Omega$.

2. We recover the density $\rho_0(z) = \frac{\overline{k_1}}{\omega_M^2(z)\, A_{\partial B}},\ z\in\Omega.$

3. Choose $\omega_\pm$ so that $\omega_\pm^2 = \omega_M^2(z) \pm a$, $a \ll 1$. Then from the formula

$$U^\infty(-\theta,\theta,\omega_+) - U^\infty(-\theta,\theta,\omega_-) = -\frac{\omega_M^2(z)}{\overline{k_1}} |B|\, [V(z,\theta,\omega_M(z))]^2 + O(a)$$

we recover $V(z,\theta,\omega_M(z))$ up to a sign.

4. Recover $k_0(z), z\in\Omega$, using numerical differentiation: $k_0^{-1}(z) = -\frac{\nabla\cdot(\rho_0^{-1}\nabla V(z,\theta,\omega_M(z)))}{\omega_M^2(z)\ V(z,\theta,\omega_M(z))}$.

Solution of the inverse problem using bubbles-Disadvantages and Solutions

- Possible zeros of the total fields $V(z, \theta, \omega_M(z))$:

  Answer: Use multiple directions of incidence θ.

- Numerical differentiation:

  Answer: Use two injected bubbles which are close to each other.

  We can recover not only the total field V but also the Green's function G_{ω_M} on the 'centers' of the two bubbles.

  From the singularities of G_{ω_M}, we recover the bulk k_0.

  Idea of the proof: use the Foldy-Lax paradigm which is justifed for nearly resonating frequencies.

Summary on the Acoustic imaging using resonating bubbles[9]

1. Injecting single bubbles and using the generated backscattered field in one incident direction, sent at multiple frequencies, we can reconstruct the

   1. the density ρ_0 via direct and stable formulas,
   2. the bulk k_0 with numerical differentiation.

2. Injecting double and close bubbles (i.e. dimers), we can avoid the numerical differentiation.

9 A. Dabrowski, A. Ghandriche and M. Sini, Mathematical analysis of the acoustic imaging modality using bubbles as contrast agents at nearly resonating frequencies. arXiv:2004.07808.

Photo-Acoustic Imaging Using Resonating Nanoparticles

Photo-acoustic imaging using nanoparticles-A general model

Let E, $\boldsymbol{T}$ and p stand respectively for the electric field, the heat temperature and the acoustic pressure.

The Photo-acoustic experiment is based on the following model coupling these three quantities:

$$\begin{cases} curl\ curl\ E - \omega^2\, \varepsilon\, \mu_0\, E = 0, \quad E := E^s + E^i, \text{ in } \mathbb{R}^3, \\ \rho_0 c_p \dfrac{\partial \boldsymbol{T}}{\partial t} - \nabla \cdot \kappa \nabla \boldsymbol{T} = \omega\, \Im(\varepsilon)\, |E|^2\, \delta_0(t), \text{ in } \mathbb{R}^3 \times \mathbb{R}_+, \\ \dfrac{1}{c^2} \dfrac{\partial^2 p}{\partial t^2} - \Delta p = \rho_0\, \beta_0\, \dfrac{\partial^2 \boldsymbol{T}}{\partial t^2}, \text{ in } \mathbb{R}^3 \times \mathbb{R}_+, \end{cases}$$

where ρ_0 is the mass density, c_p the heat capacity, κ is the heat conductivity, c is the wave speed and β_0 the thermal expansion coefficient. To the last two equations, we supplement the homogeneous initial conditions:

$$\boldsymbol{T} = p = \frac{\partial p}{\partial t} = 0, \text{ at } t = 0.$$

The $2D$ mathematical model is [10]

$$\begin{cases} \partial_t^2 p(x,t) - c_s^2(x)\Delta_x p(x,t) & = & 0 \quad in \quad \mathbb{R}^2 \times \mathbb{R}^+. \\ p(x,0) & = & \frac{\omega\,\beta_0}{c_p}\Im(\varepsilon)(x)\,|E_3|^2(x), \quad in \quad \mathbb{R}^2 \\ \partial_t p(x,0) & = & 0 \quad in \quad \mathbb{R}^2 \end{cases} \tag{4.1}$$

here c_s is the velocity of sound in the medium that is smooth and $c_s - 1$ is supported in a smooth and compact set Ω. The constants β_0 and c_p are known and ω is an incident frequency.

The source $u := E_3$, in the Transverse-Electric regime, is solution of:

$$\begin{cases} \Delta u + \omega^2 \mu_0 \varepsilon\, u = 0 \quad \text{in } \mathbb{R}^2, \\ u(x) := u^s(x) + e^{i\,\omega\sqrt{\mu_0\varepsilon_0}\,x} \\ u^s \text{ satisfies the S.R.C..} \end{cases} \tag{4.2}$$

where $\varepsilon = \varepsilon_1$ inside D, $\varepsilon = \varepsilon_0$ outside D and $\varepsilon_0 = 1$ outside Ω $\quad (D \subset \Omega)$.

10 F. Triki, M. Vauthrin. Mathematical modelization of the Photoacoustic effect generated by the heating of metallic nanoparticles. (2018).

Photo-acoustic imaging using nanoparticles-II

The goal is to recover ε in Ω from the measure of the pressure $p(x,t),\ x \in \partial\Omega$ and $t \in (0,T)$ for large enough T.

1. Acoustic Inversion: Recover the source term $\Im(\varepsilon)(x)\,|u|^2(x),\ x \in \Omega$, from the measure of the pressure $p(x,t),\ x \in \partial\Omega$ and $t \in (0,T)$.
2. Electromagnetic Inversion: Recover the permittivity $\varepsilon(x),\ x \in \Omega$ from $\Im(\varepsilon)(x)\,|u|^2(x),\ x \in \Omega$.

The data (i.e. the pressure) is collected:

- Before injecting any particle. (Ammari, Arridge, Bal, Stefanov, Scherzer, Seo, Uhlmann and many other contributors) using multiple internal data for suitable incident waves.
- After injecting a single particle. (Triki-Vauthrin, with plasmonic nanoparticles).
- After injecting a double (and close) particles.
- After injecting a cluster of particles.

Some Known Acoustic Inversions. Natterer's book and Kuchment-Kunyansky (EJAM-2008).

1. If the speed of propagation c_s is constant and Ω is a disc of radius R, then

$$\Im(\varepsilon)(x)\,|u|^2(x) = \frac{1}{2\pi R}\int_{\partial\Omega}\int_0^{2R}(\partial_r\, r\,\partial_r M(\Im(\varepsilon)\,|u|^2))(p,r)\,\log(|r^2-|x-p|^2|)\,dr\,d\sigma(p) \tag{4.3}$$

where

$$M(\Im(\varepsilon)\,|u|^2)(x,r) = \frac{2\omega\beta_0}{c_p\pi}\int_0^{c_s r}\frac{p(x,t)}{\sqrt{r^2-t^2}}\,dt. \tag{4.4}$$

2. Otherwise (under certain conditions as the non-trapping one)

$$\Im(\varepsilon)(x)\,|u|^2(x) = \frac{c_p}{\omega\,\beta_0}\sum_k(\Im(\varepsilon)(x)\,|u|^2)_k\,\psi_k(x)$$

where

$$(\Im(\varepsilon)(x)\,|u|^2)_k = \lambda_k^{-2}g_k(0) - \lambda_k^{-3}\int_0^\infty \sin(\lambda_k t)\,g_k''(t)\,dt \tag{4.5}$$

with

$$g_k(t) = \int_S p(x,t)\,\overline{\frac{\partial\psi_k}{\partial\nu}(x)}\,dx \tag{4.6}$$

and (λ_k,ψ_k) is the sequence of eigen-elements of $-c_s^{-2}(x)\Delta$ with zero DBC in $\partial\Omega$.

Let the permittivity $\varepsilon_0(\cdot)$, of the medium, be $W^{1,\infty}-$smooth in Ω and the permeability μ_0 to be constant and positive.

Here, we assume that the injected nanoparticles enjoy the properties:

$$\Re\varepsilon_p \sim a^{-2}|\log(a)|^{-1} \quad \text{and} \quad \Im\varepsilon_p \sim a^{-2}|\log(a)|^{-1-h-s}, \quad s \geq 0.$$

The frequency of the incidence ω is chosen close to the dielectric resonance ω_{n_0}:

$$\omega_{n_0}^2 := \left(\mu_0\, \varepsilon_p\, \lambda_{n_0}\right)^{-1},$$

as follows

$$\omega^2 := \omega_{\pm}^2 := \Re(\omega_{n_0}^2)(1 \pm |\log(a)|^{-h}), \quad 0 < h < 1 \tag{4.7}$$

where λ_{n_0} is an eigenvalue of the Newtonian operator acting as:

$$A_0 u(x) := \int_D -\frac{1}{2\pi} \ln(|x-y|) u(y) dy.$$

Let $x \in \partial\Omega$ and $t \geq diam(\Omega)$. Under the condition $0 \leq s < \max\{h, 1-h\}$, we have the following expansions of the pressure:

1. *Injecting one nanoparticle*. In this case, we have the expansion

$$(p^+ + p^- - 2p_0)(t,x) = \frac{-t\,\omega\,\beta_0}{c_p\,(t^2 - |x-z|^2)^{3/2}}\, 2\,\Im(\varepsilon_p) \int_D |u_1(x)|^2 dx + \mathcal{O}\left(|\log(a)|^{\max(-1,2h-2)}\right). \quad (4.8)$$

2. *Injecting two close dielectric nanoparticles.* We have the following expansion

$$(p^+ + p^- - 2p_0)(t,x) = \frac{-t\,\omega\,\beta_0}{c_p\,(t^2 - |x-z|^2)^{3/2}}\, 4\,\Im(\varepsilon_p) \int_D |u_2(x)|^2 dx + \mathcal{O}\left(|\log(a)|^{\max(-1,2h-2)}\right). \quad (4.9)$$

where D is any one of the two nanoparticles.

Acoustic Inversion

Measuring $p^{+}(x,t)$, $p^{-}(x,t)$ and $p_0(x,t)$ for

two single points $x_1 \neq x_2$ in $\partial\Omega$ at two single times $t_1 \neq t_2$,

we can

1. localize the center of the injected single nanoparticle z and estimate $\int_D |u_1(x)|^2 dx$.

2. estimate the center of the two injected nanoparticles z_1, z_2 (but we do not distinguish them). In addition, we can estimate $\int_D |u_2(x)|^2 dx$. Here D is any of the two nanoparticles.

Electromagnetic Inversion I

Injecting one nanoparticle. In this case, we have the following approximation

$$\int_D |u_1|^2(x)dx = \frac{|u_0(z)|^2(\int_D e_{n_0}(x)dx)^2}{|1-\omega^2\mu_0\varepsilon_p\lambda_{n_0}|^2} + \mathcal{O}(a^2). \tag{4.10}$$

Hence, we can extract the internal phaseless information $|u_0(z)|$. Recall that u_0 is solution of

$$\Delta u_0 + \omega^2\mu_0\varepsilon u_0 = 0. \tag{4.11}$$

This means that measuring before and after injecting one nanoparticle and scanning Ω with such nanoparticles, we transform the photo-acoustic problem to the

inverse problem of reconstructing ε from internal phaseless data $|u_0|$ with u_0 solution of (4.11).

Electromagnetic Inversion II

Injecting two closely spaced nanoparticles located at z_1 and z_2. In this case, we have at hand

$$\int_D |u_1|^2(x)dx \quad \text{and} \quad \int_D |u_2|^2(x)dx.$$

Based on the Foldy-Lax approximation for frequencies near resonances, we derive the following expansion

$$\log(|k|)(z) = 2\pi\gamma - \frac{\frac{\int_D |u_2|^2(x)dx}{\int_D |u_1|^2(x)dx} - (1 - C\Phi_0)^2}{\frac{\int_D |u_2|^2(x)dx}{\int_D |u_1|^2(x)dx} - 2(1 - C\Phi_0)} + O(|\log(a)|^{\max\{h-1, 1-2h\}}), \quad a \ll 1, \tag{4.12}$$

where γ is the Euler constant, $\Phi_0 := -\frac{1}{2\pi} \ln|z_1 - z_2|$ and

$$\mathbf{C} := \int_D [\frac{1}{\omega^2 \mu_0 \Re\varepsilon_p} I - A_0]^{-1}(1)(x)dx = \frac{\omega^2 \mu_0 \Re\varepsilon_p}{1 - \omega^2 \mu_0 \Re\varepsilon_p \lambda_{n_0}} \left(\int_D e_{n_0}(x)dx \right)^2 + O(|\log(a)|^{-1}), \quad a \ll 1.$$

As

$$|k|(z) = \omega^2 |\varepsilon_0| \mu_0 = \omega^2 \left(|\varepsilon_r|^2 + \frac{|\sigma_\Omega|^2}{\omega^2} \right)^{1/2} \mu_0, \tag{4.13}$$

then using two different resonances ω_{n_0} and ω_{n_1}, we can reconstruct both the permittivity $\varepsilon_r(z)$ and the conductivity $\sigma_\Omega(z)$.

Imaging using a cluster of contrast agents-I

We inject a cluster of contrast agents $(D_m, \varepsilon_m, \mu_0), m = 1, 2, ..., M$ inside Ω.

Assumptions:

1. We have both $\Re\varepsilon_m \sim \overline{\varepsilon_m}_r a^{-2}$ and $\Im\varepsilon_m \sim \overline{\varepsilon_m}_i a^{-2+h}$, with $h \in (0,1)$.
2. $1 - \frac{\omega_{n_0}^2}{\omega^2} = l_M a^h$, with $l_M \neq 0$ and $h \in (0,1)$.
3. There exists a function K such that

$$\frac{1}{[a^{-1+h}]} \sum_{j \neq m}^{[a^{-1+h}]} \frac{f(z_j)}{|z_j - z_m|} - \int_\Omega \frac{f(z)}{|z - z_m|} K(z) dz = o(1) \|f\|_{C^0(\Omega)}, \text{uniformly for } z_j \text{ and as } a \ll 1. \quad (4.14)$$

This means we use a cluster of M particles of the order $M \sim a^{h-1}$, $0 < h < 1$ and $a \ll 1$.

Imaging using a cluster of contrast agents-II

Under these assumptions, we have $u(x,\theta) - u_K(x,\theta) = o(1)$, as $a \ll 1$. where

$$\left(\Delta + \omega_{n_0}^2 \varepsilon_K(x)\mu_0\right) u_K^t = 0, \text{ in } \mathbb{R}^3, \quad u_K^t = u_K^s + e^{i\kappa_0 x\cdot\theta}, \quad \frac{\partial u_K^s}{\partial |x|} - i\kappa_0 u_K^s = o\left(\frac{1}{|x|}\right), \; |x| \to \infty, \tag{4.15}$$

with $\Re\varepsilon_K := \Re\varepsilon - K\frac{|B|}{l_M}\overline{\varepsilon_m}_r\chi_\Omega$. and $\Im\varepsilon_K = \Im\varepsilon + K\frac{|B|}{l_M}\overline{\varepsilon_m}_r\chi_\Omega$.

Choosing $l_M > 0$, we have

$$\Re\varepsilon_K(x) < 0, \quad \text{for} \quad x \in \Omega \quad \text{and} \quad \varepsilon_K(x) - \varepsilon \text{ can be large .}$$

We can use $l_M \ll 1$ or $K \gg 1$ to enhance these contrasts.

Imaging using a cluster of contrast agents-III.

1. From the measured pressure after injecting the cluster, we recover the pressure due to the effective medium ε_K (via homogenization). The advantage here is that we use a sparse cluster of nanoparticles with nearly resonating frequencies however.

2. From this data, we recover $\Im \varepsilon_K \, |u_K|^2$ and hence $|u_K|^2$ as $\varepsilon_K(x) - \varepsilon$ is large and known.

3. This phaseless total internal field corresponds to a locally coercive Helmholtz wave propagator. By homogenization we switch the sign of the index of refraction as for metamaterials (in material sciences).

4. Due to coercivity, the corresponding least square functional has a positive second Gateau-derivative. Hence it is a convex functional. Already observed by I. Knowles.

5. The slope of the functional is sharper as $l_M \ll 1$ or $K \gg 1$.

Summary and perspectives

1. Imaging with contrast agents is among the promising modalities that are at the cutting edge of modern medical imaging.

2. We have a clear correspondence between the critical scales of the contrasting materials and the actual resonances.

3. Using nearly resonating frequencies provides simple and direct links between the measured data and the background coefficients.

4. We have demonstrated this in two frameworks: Acoustic Bubbles and Electromagnetic Nanoparticles in their simplest models however.

5. Combination of imaging techniques with homogenization might be applied successfully to different modalities as Raman Imaging and MREIT.

THANK YOU

More details by email at mourad.sini@oeaw.ac.at or in www.//people.ricam.oeaw.ac.at/m.sini/